

Damage characterization in a bar using guided waves

Annamaria Pau¹, Fabrizio Vestroni¹

¹*Department of Structural and Geotechnical Engineering, Sapienza University of Rome, Italy*
E-mail: annamaria.pau@uniroma1.it, vestroni@uniroma1.it

Keywords: Wave propagation, damage identification, one-dimensional waveguides.

SUMMARY. The waveguide geometry of numerous structures used in civil and mechanical engineering can be exploited for the use of guided waves in damage detection. The present study examines the response of a bar to an impulsive force along its axis and points out the differences emerging when the bar has a damage of notch-type. Relationships between the damage parameters and the amplitude and time-delay of the reflected and transmitted waves are exploited to formulate a damage characterization procedure. The presented procedure is tested analytically and experimentally in different damage configurations.

1 INTRODUCTION

In recent years, methods based on wave propagation gained increasing attention for the nondestructive evaluation and health monitoring of various kinds of onedimensional waveguides, such as pipes, beams, ropes, multiwire strands, rockbolts. The interaction of guided waves with discontinuities in the waveguide is a topic that has stimulated a great deal of interest. The ability of waves to locate cracks in onedimensional waveguides is widely documented and the effect of defect size on the reflection and transmission has been investigated by many researchers [1]-[2].

Significant efforts have been devoted to ensure that only the desired propagation modes are excited and work in non-dispersive regions. The dispersion characteristics and cutoff frequencies of elastic waves generated by an impulse in various waveguides were experimentally observed by [1], providing useful considerations for the choice of the wave frequencies and propagating modes that are more favorable for application to a given geometry in nondestructive evaluation.

Initial practical testing on pipes was done using the longitudinal mode [3] in its nondispersive region over the cutoff frequency. However, later testing employed the torsional mode. This has the advantage that there is no other axially symmetric torsional mode in the frequency range, in contrast to the longitudinal mode, so axially symmetric torsional excitation will only excite one propagation mode [4]. Here, the reflection coefficients from crack and notches of varying depth, circumferential and axial extent when the torsional mode is incident are determined using FE models, with a comparison to experimental results. In the case of notches having finite axial extent, interferences from the start and end of the notch cause a variation of the amplitude of the reflected signal as a function of the notch length. FE models are used to generalize the results previously obtained [5], by deriving approximate formulae relating the reflection coefficients to the notch characteristics.

As shown in a recent paper [6] collecting a wide number of references, in the majority of the literature testing is restricted to low frequencies, which may be sufficient if one is interested in locating the defect and not in characterizing it. The objective of the present study is examining the problem of damage identification of notch type in onedimensional axial waveguides in selected operative cases, focusing the attention on the defect characterization. The direct problem is studied, showing that the wave generated by an impulsive force interacts with the two changes in the cross section, generating other waves in the bar. Relationships exist between the amplitude and time delay of transmitted and reflected waves and the damage characteristics. Hence, the inverse problem of

damage characterization can be solved by using the experimental time-histories.

A procedure of damage identification based on the comparison between analytical and experimental quantities is presented, which uses both reflected and transmitted signals. The procedure is tested using pseudo-experimental and experimental data in different damage configurations.

2 MODELLING OF THE IMPULSIVE RESPONSE IN A DAMAGED BAR

The response of a cylindrical damaged bar to an impulsive force along the longitudinal axis is considered. The damage consists in a sharp reduction of the cross-section of a certain length. The damage is then characterized by three parameters: position x_d , extension a and ratio between the areas of the cross-section in the damaged and undamaged zones $r = A_2/A_1$ (Figure 1).

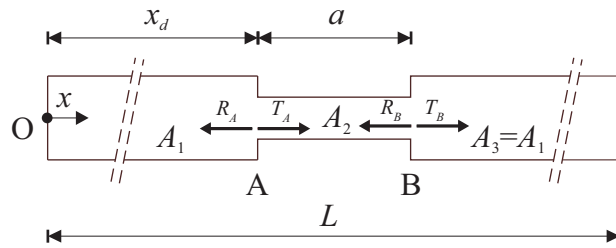


Figure 1: Scheme of the damaged bar.

The equation of motion for the bar is the familiar wave equation:

$$\frac{\partial^2 u}{\partial x^2} = \frac{1}{c_0^2} \frac{\partial^2 u}{\partial t^2} \quad (1)$$

where u is the displacement in the axis direction and

$$c_0 = \sqrt{\frac{E}{\rho}} \quad (2)$$

is the wave propagation velocity, E Young's modulus and ρ mass density. To equation (1) the D'Alembert's solution pertains:

$$u(x, t) = f\left(t - \frac{x}{c_0}\right) + g\left(t + \frac{x}{c_0}\right) \quad (3)$$

so that longitudinal wave propagate at the velocity c_0 without distortion.

The response of a semi-infinite bar to a transient load applied at its free end is the solution to equation (1) with the following initial and boundary conditions:

$$u(x, 0) = 0 \quad \frac{\partial u(x, 0)}{\partial t} = 0 \quad EA \frac{\partial u(0, t)}{\partial x} = p(t), \quad (4)$$

where A is the area of the cross section. The solution to this problem is well known [7]:

$$u(x, t) = f\left(t - \frac{x}{c_0}\right) = f(\tau) = -\frac{c_0}{EA} \int_0^\tau p(\xi) d\xi. \quad (5)$$

The damaged bar can be divided into three regions, each with constant cross-section A_i , according to Figure 1. The stress wave caused by the impulsive force interacts with the two changes in the cross section (A and B in Figure 1), generating other waves in the bar. The amplitude of these waves is indicated in the following formulae as R for reflected and T for transmitted waves, with a subscript defining the change of section from which the wave is originating, as in Figure 1.

By exploiting the D'Alembert solution, the time-history of the reflected $R(x, t)$ and $T(x, t)$ transmitted waves, respectively to regions 1 and 3, can be written as a superposition of wave components with amplitudes governed by R_{A_i} and T_{B_i} :

$$R(x, t) = \sum_{i=1}^{\infty} R_{A_i} f\left(t + \frac{2}{c_0}[x_d - x + a(i-1)]\right) \quad (6)$$

$$T(x, t) = \sum_{i=1}^{\infty} T_{B_i} f\left(t - \frac{1}{c_0}[x + 2a(i-1)]\right). \quad (7)$$

R_{A_i} and T_{B_i} can be expressed as a function of r by writing the boundary conditions, i.e. equilibrium of forces and continuity of velocities where the change of section occurs [7]. Equations 6 and 7 are expressions valid for different kinematic response quantities provided that the appropriate f is used. The values of R_{A_i} and T_{B_i} rapidly decrease when i increases. The first three of these coefficients are represented in Figure 2 as a function of r . The picture shows that R_{A_2} is always negative, whereas T_{B_2} always sums to T_{B_1} . In the range of interest of damage intensity, which is $0.5 < r < 1$, the coefficients with $i > 2$ are negligible for R and $i > 1$ for T .

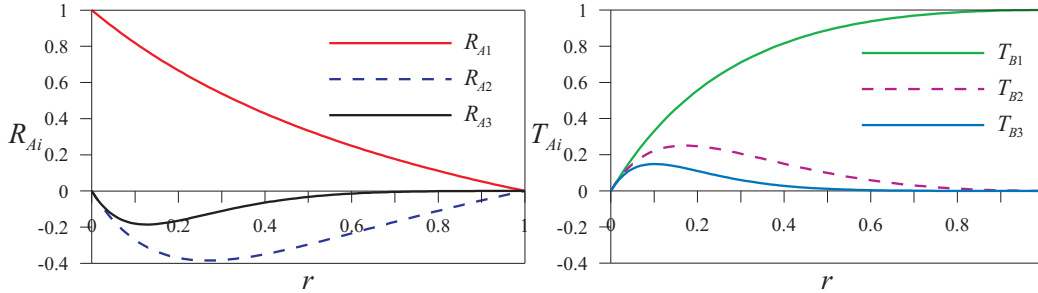


Figure 2: Reflection and transmission coefficients.

Figure 3a represents with a continuous line the acceleration time-histories at the abscissae x_1 , before the notch, and x_2 , after the notch, due to a wave generated by an impulse at $x = 0$. The time-histories are obtained from equations (6), assuming $i = 1, 2$ and (7), assuming $i = 1$. These reflection and transmission coefficients alone provide a satisfactory approximation of the acceleration time-histories. This is proved in Figure 3a that reports also a comparison with a FE model,

showing that the curves of the two models superimpose. Figure 3b represents the different roles of the single wave components in the time-history. Each of them is reported with the same colors and line styles as those used in Figure 2. According to their magnitude and sign these components interact to provide the time-history of Figure 3a.

Figure 4 shows the acceleration time-histories of the reflected wave for different ratios between minimum wavelength of the excitation λ and damage extension a . R_{A1} and R_{A2} interact in destructive and constructive interference as a function of the ratio λ/a . When a small λ is used (Figure 4a,b) they are well resolved, but when λ is large (Figure 4f), the destructive interference tends to hide the presence of the notch. Therefore, it is mandatory to use a signal having a minimum wavelength of the same order of magnitude of the notch extension. The smaller the extension, the smaller λ is needed. This fact poses technological challenges in damage identification of small notches. For intermediate λ (Figure 4c-e), the interference can be constructive. As a consequence of the interference, the maximum amplitude of the reflected wave is not sufficient to solve the inverse problem of damage identification. In fact, the same value of amplitude can be found for a broad range of r as a consequence of destructive and constructive interference. In the transmitted signal, the importance of T_{B2} tends to decrease for $r > 0.15$, as shown in Figure 2b.

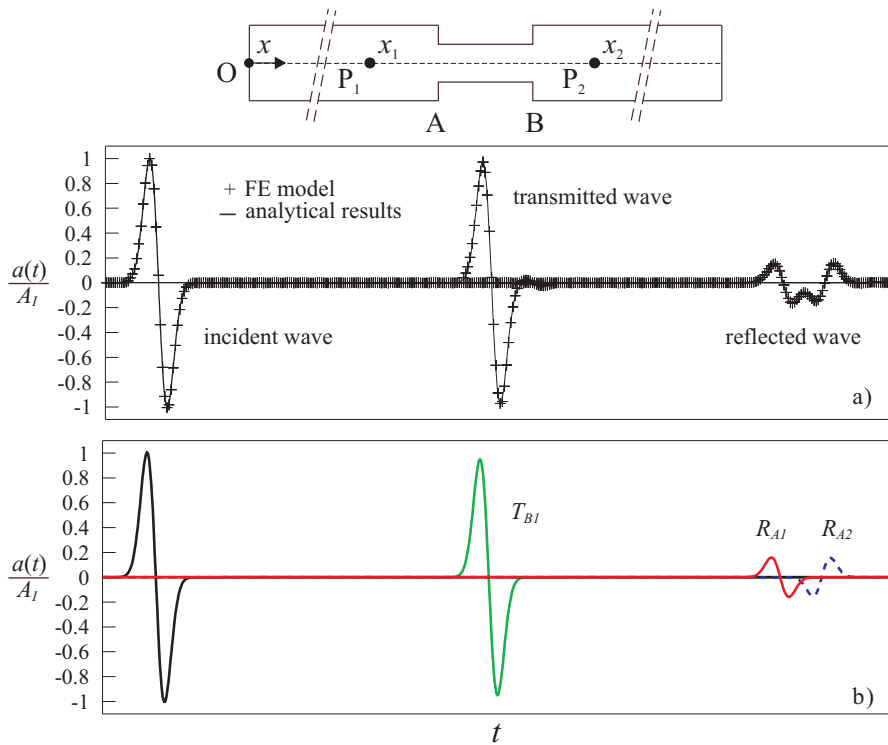


Figure 3: Time-histories of acceleration at points P_1 and P_2 : comparison between FE model and analytical results a) and contribution of the different wave terms to the time-history b).

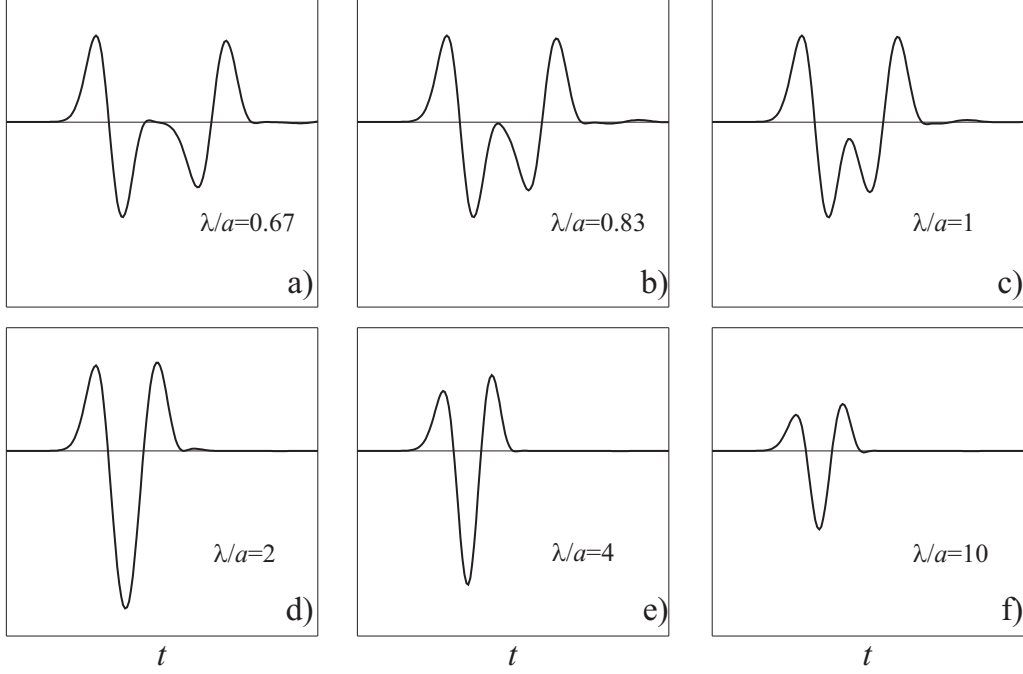


Figure 4: Time-histories of the reflected wave for different ratios λ/a .

3 DAMAGE IDENTIFICATION PROCEDURE

In real cases, the response is strongly dependent on damping. This must be taken into account in order to formulate an effective identification procedure. The damping can be experimentally measured on the undamaged bar. If a spatial exponential decay is assumed for the wave amplitude:

$$A(x) = A_0 \exp(-\xi x), \quad (8)$$

ξ can be determined by the ratio:

$$\xi = \frac{1}{x} \ln \frac{A_0}{A(x)} \quad (9)$$

between the wave amplitudes in two points at a relative distance x . In this way, the amplitude decrement due to damping can be isolated from the reflection and transmission phenomena.

Then, considering only the terms $i = 1, 2$ in (6) and $i = 1$ in (7), the model of the response is, for the reflected and transmitted wave:

$$R(x_1, t) \simeq R_{A1} f\left(t + \frac{2}{c_0}[x_d - x_1]\right) e^{-2\xi[x_d - x_1]} + R_{A2} f\left(t + \frac{2}{c_0}[x_d - x_1 + a]\right) e^{-2\xi[x_d - x_1 + a]} \quad (10)$$

$$T(x_2, t) \simeq T_{B1} f\left(t - \frac{x_2}{c_0}\right) e^{-\xi x_2}, \quad (11)$$

where $f(t)$ is the shape function of the incident wave.

By using the expressions (10) and (11), the inverse problem of damage characterization can be formulated as follows: assuming that $f(t)$, $R(x_1, t)$, $T(x_2, t)$ and ξ are known, determine a , r and x_d . An important point in the procedure consists in defining the function f , which depends on the forcing function, according to equation (5). In experimental tests, the use of transient loads generated by an instrumented hammer is very common. The time-history of this kind of excitation is well approximated by the Gaussian function:

$$p(t) = P e^{-b(t-t_0)^2}, \quad (12)$$

where b is a coefficient that governs the impulse duration and t_0 the starting of the phenomenon in time. Considering the fact that acceleration is a response quantity easy to measure and recalling equation (5), the response $a(x, t)$ can be written as:

$$a(x, t) = -\frac{c_0}{EA} \frac{dp}{dt} = -\frac{2c_0 P b}{EA} (t - t_0) e^{-b(t-t_0)^2}, \quad (13)$$

from which the function representing the incident wave is derived:

$$f(t) = -A_I (t - t_0) e^{-b(t-t_0)^2}. \quad (14)$$

Here, the presented procedure of damage characterization is based on the comparison between analytical and experimental acceleration time-histories. The procedure consists in determining the damage parameters in a prescribed order, that enables to obtain a unique solution. First of all, the damping coefficient ξ is determined from the response of the undamaged bar, by measuring the wave amplitudes at two locations and determining ξ from equation (9). Then, an optimal estimate of damage intensity r is obtained from the amplitude of the transmitted signal (11):

$$T_{B1} = \frac{4r^2}{(1+r)^2}. \quad (15)$$

A unique value of r corresponds to T_{B1} in the range $0 < r < 1$, as can be seen from Figure 2b. This is not true for all values of r , however, the values of r outside the range $0 < r < 1$ are not physically consistent. Finally, after having calculated R_{A1} and R_{A2} , which are functions of r according to:

$$R_{A1} = \frac{1-r}{1+r} \quad R_{A2} = \frac{4r(r-1)}{(1+r)^3}, \quad (16)$$

the extension a and position x_d are determined from the reflected signal (10).

4 EXPERIMENTAL SETUP AND RESULTS

The experiments were carried out at the Laboratory of the Department of Structural and Geotechnical Engineering, Sapienza University of Rome. A PVC bar with circular cross section is used. Its geometrical and mechanical properties are listed in Table 1. The bar is suspended by elastic wires to approximate free conditions. The geometry of the experimental setup is depicted in Figure 5. The structure is excited by an instrumented hammer at its right free end and its response measured by three uniaxial piezoelectric accelerometers (Ch0, Ch1, Ch2). These have a bandwidth ranging from 0.25 to 8000 Hz, a dynamic range of ± 5000 g and a sensitivity of 0.9 mV/g. They were connected to a data acquisition system with 16 bit A/D converter, and anti-aliasing filters.

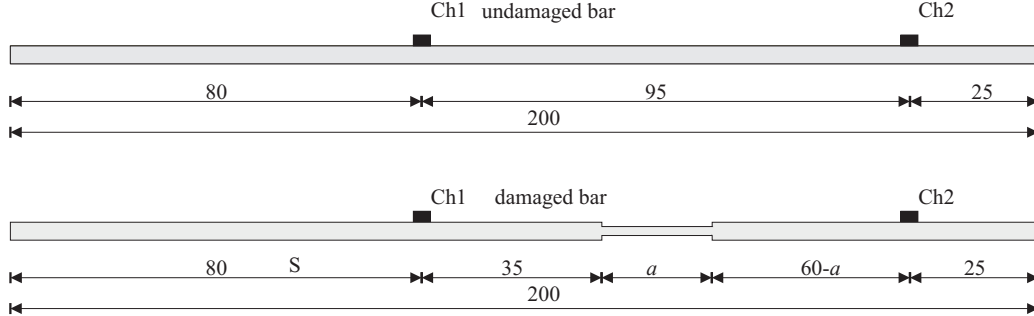


Figure 5: Experimental set-up, lengths in [cm].

The bar was tested in three different damage configurations, which are made by removing material so that the transverse section of the damaged part preserves circular and the axis of the bar straight. The configurations are described in Table 2, where D_d indicates the diameter of the damaged part, and differ for intensity and extension of damage. The extension of the notch is scaled in order to take into account the fact that the minimum wavelength contained in the signal generated with the hammer is about 10 cm. The scaling of the notch is only due to technical limitations of the present setup but does not affect the investigation on the effectiveness of procedure. If shorter wavelength had been used, smaller notches would have been detected.

Table 1: Geometrical and mechanical properties of the PVC bar

$E[MPa]$	$\rho[kg/m^3]$	$L[cm]$	$D[cm]$	$c_0[m/s]$
4150	1400	200	2	1721.71

The comparison between the experimental response of the undamaged and damaged bars shows that in the latter, the wave reflections from the discontinuities clearly appear. This is shown in Figure 6, which presents the experimental time-histories of accelerations recorded at Ch1 and Ch2 for the undamaged (a) and damaged bar (b). A reflected signal appears in the time-history of Ch1. When comparing the transmitted and reflected wave in the damaged case, also the dependence of the response on the damage intensity and extension evidently appears. In fact, the amplitude of the transmitted wave from a damage with greater intensity is smaller, as expected according to the analytical results and shown in Figure 7a,b. With regard to the reflected wave, when the extension of the notch is small, for the present impulse, constructive interference takes place (Figure 7c), but when the two discontinuities are sufficiently far, the two reflections are resolved (Figure 7d). This phenomenon had been predicted by the analytical model too.

First of all, the spatial exponential decay ξ is determined based on the response of the undamaged bar. The unknown ξ is obtained by curve-fitting the experimental response to the model equation (14). A mean value of $\xi = 0.69$ is obtained with a coefficient of variation $c_v = 6.42\%$ calculated on 10 repetitions of the test. When ξ is known, the first step is the evaluation of the damage intensity from the transmitted wave. By minimizing the difference between the experimental transmitted

wave and the analytical response, equation (11), an amplitude T_{B1} is obtained, from which r is determined, according to equation (??). Figure 8b shows that there is a good agreement between the experimental and the curve-fitted response. For the sake of brevity, this comparison is illustrated for the case D4 only. Then, the difference between experimental and analytical reflected wave, expressed by equation (10), is minimized, which enables to evaluate the optimal values of x_d and a . Also for the reflected wave a good agreement between the experimental and curve-fitted response is found, as is shown in Figure 8a.

Table 2: Geometrical characteristics of the notches

	$D1$	$D3$	$D4$
D_d [cm]	1.7	1.4	1.4
r	0.72	0.50	0.50
a [cm]	10	10	15

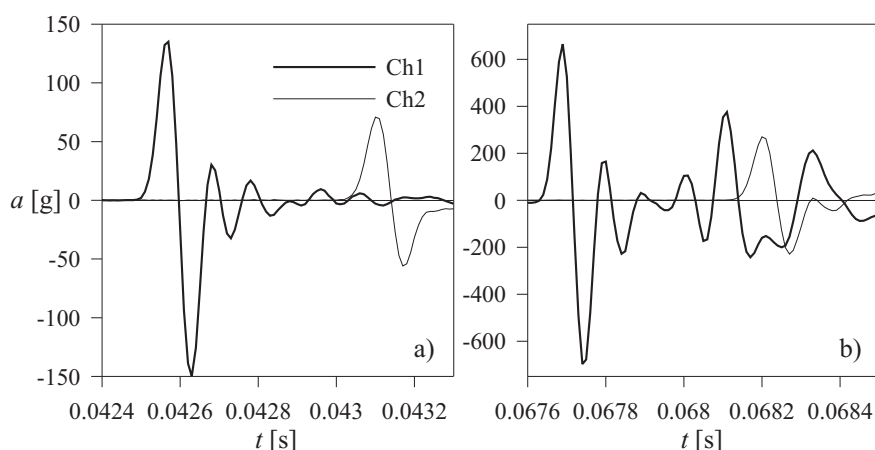


Figure 6: Comparison of two experimental time-histories in the undamaged a) and damaged D4 b) cases.

As a whole, the identified characteristics of the damage agree with the actual values. This is shown in Table 3, that reports the comparison between real and identified (with subscript i) damage characteristics. The error is of some percent units and has the same order of magnitude for the different identified parameters.

Table 3: Identified damage characteristics

	D_d	D_{di}	% err	x_d	x_{di}	% err	a	a_i	% err
D1	1.7	1.6	5.9	35	36.8	5.2	10	10.7	6.7
D3	1.4	1.2	14.3	35	36.7	9.9	10	13.7	9.9
D4	1.4	1.2	14.3	35	37.4	6.9	15	14.5	2.8

5 CONCLUSIONS

The transient response of one-dimensional bar excited by an impulsive axial force is sensitive to the presence of a discontinuity. This sensitivity can be exploited to define a damage identification procedure based on a D'Alembert's model of the response. Here, this procedure has been presented for the case of a longitudinally excited bar. The main damage characteristics, which are intensity, position and extension are determined by minimizing the difference between the model and experimental response. A good agreement was found between real and identified values. This is an interesting result that let the presented damage identification procedure emerge as an effective technique of damage characterization.

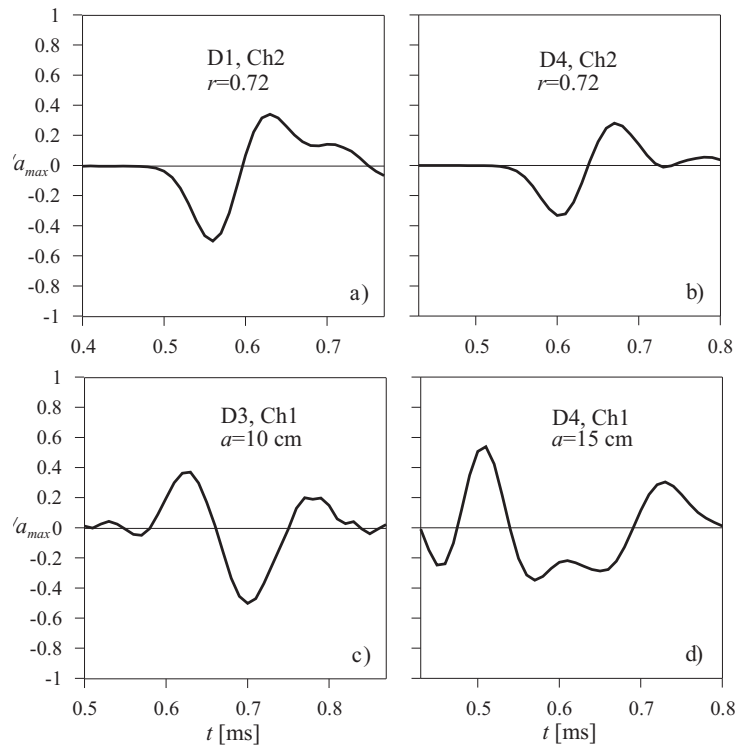


Figure 7: Experimental time-histories of transmitted a,b) and reflected c,d) waves in different damage configurations.

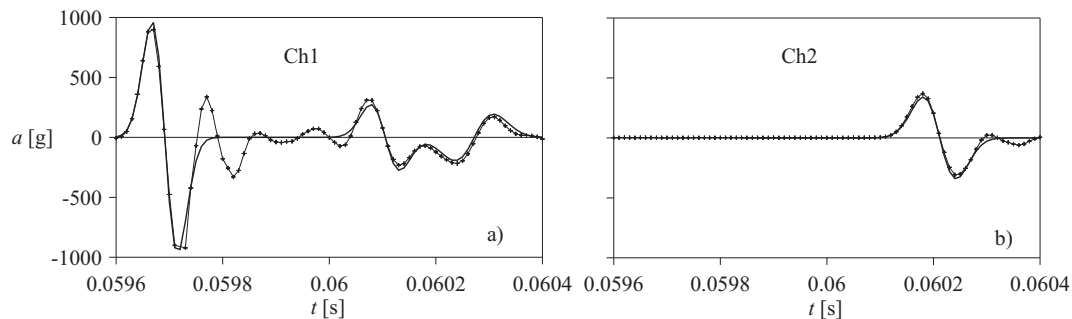


Figure 8: Comparison between analytical (bold line) experimental (line with crosses) time-histories of reflected (a) and transmitted (b) waves for the case D4.

References

- [1] H. Kwun and G. L. Burkhardt. Relationship between reflected signal amplitude and defect size in rope inspection using a transverse-impulse vibrational wave. *NDT & E International*, 24(6): 317–319, 1991.
- [2] J. F. Doyle. Determining the size and location of transverse cracks in beams. *Experimental Mechanics*, 35(3):272–280, 1995.
- [3] D. Alleyne, B. Pavlakovic, M. Lowe, and P. Cawley. Rapid long-range inspection of chemical plant pipework using guided waves. *Insight*, 43:96–93, 2001.
- [4] A. Demma, P. Cawley, M. Lowe, and A. G. Roosenbrand. The reflection of the fundamental torsional mode from cracks and notches in pipes. *Journal of the Acoustical Society of America*, 114(2):611–625, 2003.
- [5] A. Demma, P. Cawley, M. Lowe, A. G. Roosenbrand, and B. Pavlakovic. The reflection of guided waves from notches in pipes: a guide for interpreting corrosion measurements. *NDT & E International*, 37:167–180, 2004.
- [6] A. Raghavan and C. E. S. Cesnik. Review of guided-wave structural health monitoring. *The Shock and Vibration Digest*, 39(2):91–114, 2007.
- [7] J. D. Achenbach. *Wave Propagation in Elastic Solids*. Elsevier, 1973.